Received: 20 October 2019 | Revised: 25 June 2020 | Accepted: 3 August 2020

DOI: 10.1002/suco.201900440

TECHNICAL PAPER

fib CEB-FIP WILEY

Unified geometrical framework for the plastic design of reinforced concrete structures

Marina Konstantatou[1] | **Pierluigi D'Acunto**[2] | **Allan McRobie**[1] | **Joseph Schwartz**[2]

[1]Department of Engineering, University of Cambridge, Cambridge, UK

[2]ETH Zürich, Institute of Technology in Architecture, Chair of Structural Design, Zürich, Switzerland

Correspondence
Marina Konstantatou, Department of Engineering, University of Cambridge, Cambridge, UK.
Email: mk822@cam.ac.uk

Funding information
Engineering and Physical Sciences Research Council UK, Grant/Award Number: EP/L016095/1

Abstract

Although the analysis and design of structures in static equilibrium can be intuitively carried out using simple equilibrium-based methods such as graphic statics, the application of these methods to engineering problems that take into consideration specific material properties is generally limited. Within the domain of reinforced concrete, existing geometric approaches for developing stress fields and yield lines based on the theory of plasticity are especially useful. However, these approaches usually rely on iterative constructions and are generally limited to two-dimensional cases. By taking advantage of graphic statics, this article introduces the theoretical basis for an entirely geometrical method to generate discrete stress fields and yield line patterns in two- and three-dimensional reinforced concrete structures. The proposed approach is based on the use of reciprocal stress functions and the relationship between form and force diagrams.

KEYWORDS

Airy stress function, graphic statics, reciprocal diagrams, reinforced concrete, stress fields, structural analysis and design, strut-and-tie models, yield line patterns

1 | INTRODUCTION

1.1 | Objectives and contributions

This article describes the theoretical basis of a novel geometry-based framework for the analysis and design of discrete stress fields in reinforced concrete structures. The proposed method enables the direct generation of two- and three-dimensional stress fields in a continuum for specified applied loads, boundary conditions, material strength and an input strut-and-tie topology. Following a similar theoretical approach, a geometry-based method for the analysis and design of compatible yield line patterns in reinforced concrete slabs is described, and observations are made with respect to the internal and external work. In fact, it is shown how the same fundamental geometric constructions are at the core of both proposed methods. These constructions underpin the definition of stress fields in equilibrium, through the application of the lower bound theorem of plasticity theory, as well as

Discussion on this paper must be submitted within two months of the print publication. The discussion will then be published in print, along with the authors' closure, if any, approximately nine months after the print publication.

compatible yield line patterns through the application of the upper bound theorem.

The proposed framework introduces a direct, visual and intuitive analysis and design approach, which is unified for 2D and 3D cases. Moreover, given the interconnected relationship between the four reciprocal objects of graphic statics—that is, a pair of form and force diagrams and a corresponding pair of reciprocal stress functions—the approach can be applied to any of these objects since the others are then updated accordingly.[1] The applicable cases are any type of 2D truss geometries and polyhedral, plane-faced, 3D trusses. The resulting force diagrams are Maxwell 2D reciprocals for the 2D case—where form edges correspond to reciprocal perpendicular force edges and form nodes to reciprocal closed force polygons—and Rankine 3D reciprocals for the 3D case—where form edges correspond to reciprocal perpendicular force faces and form nodes to reciprocal closed force polyhedra. Preliminary results of this research have been presented in Konstantatou et al.[2]

1.2 | Outline

The remainder of this article is organized as follows. Section 2 introduces the fundamental notions that are at the base of the proposed unified geometrical framework for the plastic design of reinforced concrete structures. More specifically, Section 2.1 presents the concepts of form and force diagrams and reciprocal stress functions within the domain of graphic statics. Section 2.2 deals with current approaches for the design of strut-and-tie models and stress fields in reinforced concrete structures, while Section 2.3 is a brief overview of yield line theory in reinforced concrete slabs. Section 3 presents the proposed geometrical framework for the generation of stress fields and yield line patterns in reinforced concrete. In particular, in Section 3.1, the method for the generation of discrete stress fields is described in a detailed step-by-step manner. Section 3.2 applies the proposed framework to yield line patterns. Furthermore, it discusses the governing equations of internal and external work by pointing out how these can be expressed geometrically through polyhedral stress functions and the combination of form and force diagrams (i.e., Minkowski Sum). Section 4 presents several applications of the proposed approach to common 2D discrete stress fields (Section 4.1) and 2D yield line patterns (Section 4.4). Concerning the stress fields, extensions are shown to the continuous (Section 4.2) and the three-dimensional (Section 4.3) cases. Lastly, Section 5 comprises the concluding remarks and discussion on the applicability and advantages of the proposed framework.

2 | FUNDAMENTAL NOTIONS

2.1 | Form diagrams, force diagrams, and reciprocal stress functions

Established as an independent discipline for the analysis and design of structures in static equilibrium in the 19th century,[3–6] graphic statics is grounded on the principle of duality between reciprocal form and force diagrams. Although it lost its popularity in the first half of the 20th century, owing to the advancement of analytical mechanics, graphic statics underwent a resurgence in the 21st century thanks to the new developments in digital computing and visualization. In recent years, several approaches based on graphic statics have been proposed to address various problems in structural engineering and architectural design.[7–12] Yet, the majority of these implementations are built around iterative algorithms that do not take full account of the characteristics of the reciprocal higher dimensional stress functions, which underlie form and force diagrams. It was only recently that the fundamental role of stress functions was revealed within the domain of graphic statics.[13] In this context, particularly relevant is the Airy stress function, which was introduced by George Biddell Airy[14] to describe the inner stresses in two-dimensional continuous structures. The stress function satisfies the governing equations for equilibrium.[15] It can be regarded as a 3D surface $\varphi(x,y)$ over the 2D xy-plane that contains the structure, and which can be differentiated to give the following quantities:

$$\sigma_{xx} = \frac{\partial^2 \varphi}{\partial y^2}, \sigma_{yy} = \frac{\partial^2 \varphi}{\partial x^2}, \tau_{xy} = -\frac{\partial^2 \varphi}{\partial x \partial y} \quad (1)$$

For any twice-differentiable 3D function, these second derivatives—the local curvatures of the function—define a 2D stress field which is necessarily in equilibrium in the absence of body forces. As a result, the Airy stress function can be used for studying the static equilibrium of pin-jointed frameworks (i.e., trusses). In this case, the surface $\varphi(x,y)$ is not a continuously smooth surface but a plane-faced polyhedral surface in which the curvature is zero in the planar faces that are adjacent to each polyhedral edge while the curvature change is concentrated along the edges. In fact, 2D trusses can be seen as projections of 3D polyhedral Airy stress functions, in which the bars of the 2D structures are the projections of the polyhedral edges of the 3D stress function. The relation between Airy stress functions and equilibrium of pin-jointed frameworks was already known by James Clerk Maxwell, who refers to it in his articles on graphic

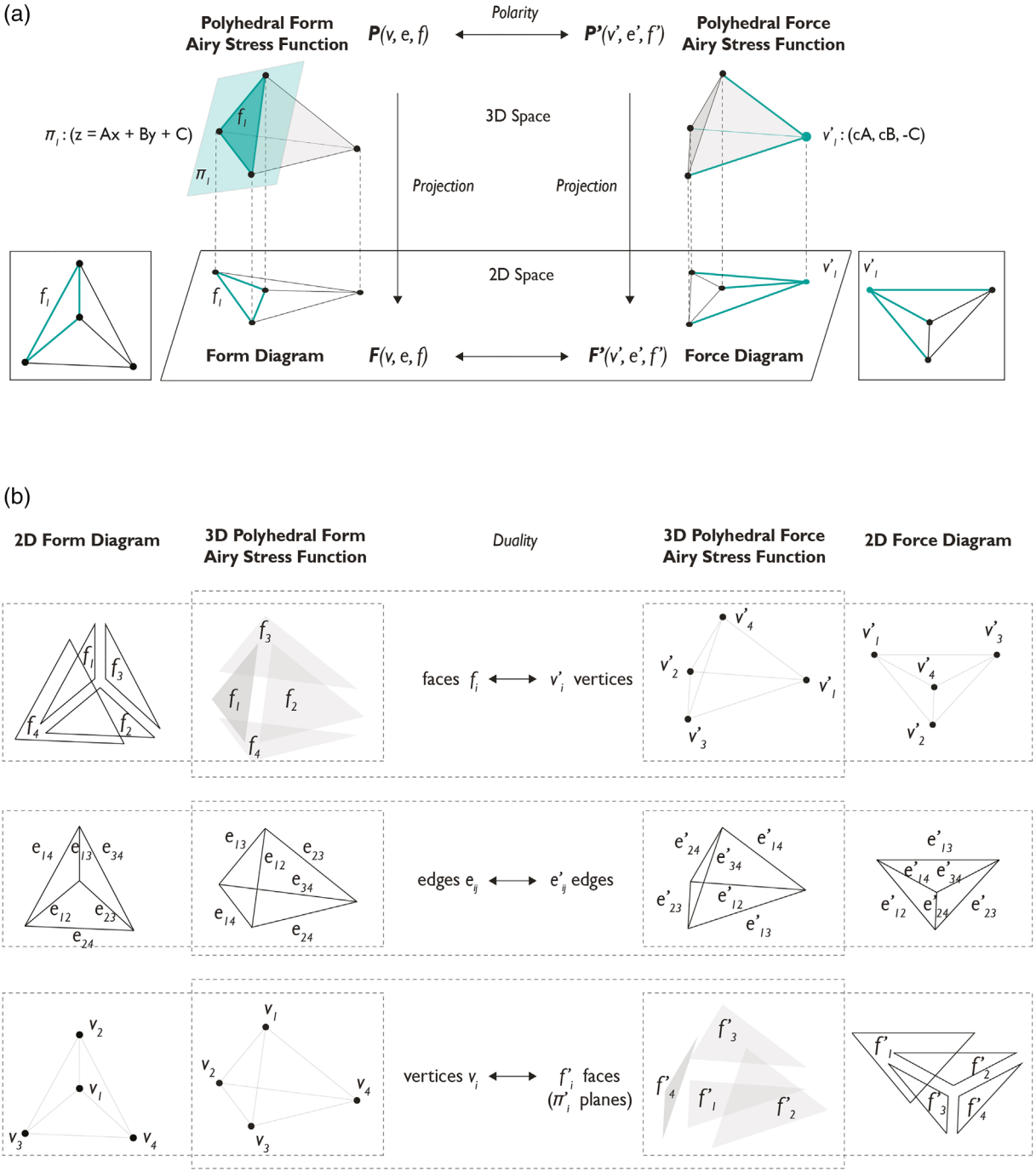

FIGURE 1 (a) Mapping between a plane π_1 containing a face f_1 of $\boldsymbol{P}(v, e, f)$ and a reciprocal vertex v'_1. This mapping is, in fact, a polar transformation which transforms a plane π_1 with equation $z = Ax + By + C$ to a point v'_1 with coordinates $(cA, cB, -C)$ and vice versa. This transformation results in a pair of reciprocal polyhedra $\boldsymbol{P}$, $\boldsymbol{P}'$ where vertices v map to faces f', edges e to edges e' and vice versa. Projecting $\boldsymbol{P}$, $\boldsymbol{P}'$ onto the plane results in a pair of 2D reciprocal diagrams $\boldsymbol{F}$, $\boldsymbol{F}'$. Following the geometrical correspondence between $\boldsymbol{P}$ and $\boldsymbol{P}'$, every vertex v of $\boldsymbol{F}$ corresponds to a closed force polygon f' in $\boldsymbol{F}'$—thus guaranteeing static equilibrium. (b) Faces f_i in $\boldsymbol{F}$ (respectively $\boldsymbol{P}$) map to reciprocal vertices v'_i in $\boldsymbol{F}'$ (respectively $\boldsymbol{P}'$); edges e_{ij} in $\boldsymbol{F}$ (respectively $\boldsymbol{P}$) map to reciprocal edges e'_{ij} in $\boldsymbol{F}'$ (respectively $\boldsymbol{P}'$). Following Maxwell's constructions,[5,16] reciprocal edges e_{ij}, e'_{ij} are perpendicular to each other and the edge length of e'_{ij} visually depicts the axial force of e_{ij}; vertices v_i in $\boldsymbol{F}$ (respectively $\boldsymbol{P}$) map to reciprocal faces f'_i in $\boldsymbol{F}'$ (respectively $\boldsymbol{P}'$). From the above dualities between reciprocal geometrical elements, it can be seen that if two faces f_1, f_2 intersect in an edge e_{12} then their corresponding reciprocal vertices v'_1, v'_2 are connected by an edge e'_{12}[1]

statics.[5,16] The dihedral angle between two adjacent faces in the 3D polyhedral Airy stress function readily defines the internal axial force of the corresponding bar in the 2D structure. Additionally, the local convexity of the function, which determines whether the edge of the polyhedron is convex or concave, defines if the corresponding bar in the structure is respectively in compression or in tension.

As shown in Figure 1a, given a 2D truss $\boldsymbol{F}$ in static equilibrium, a force reciprocal $\boldsymbol{F}'$ can be found using the following geometric procedure.[1] From the 2D truss $\boldsymbol{F}(v, e, f)$—where v are the vertices, e the edges and f the faces—the corresponding polyhedral form Airy stress function $\boldsymbol{P}(v, e, f)$ is constructed by lifting up the vertices v of $\boldsymbol{F}$ to the 3D space. Each plane π_i containing a face f_i of $\boldsymbol{P}$ is then mapped to a reciprocal point v'_i, via a *polar transformation*. The resulting points v' can be then connected to generate a reciprocal polyhedral force Airy stress function $\boldsymbol{P}'(v', e', f')$ following the connectivity of the faces f of $\boldsymbol{P}$. That is, if two faces f_1, f_2 of $\boldsymbol{P}$ intersect in an edge e_{12} then their reciprocal vertices v'_1, v'_2 of $\boldsymbol{P}'$ are connected by an edge e'_{12} in $\boldsymbol{P}'$. The Airy stress function $\boldsymbol{P}'$ can be then projected down to the 2D space to generate the force diagram $\boldsymbol{F}'(v', e', f')$. Thanks to this construction, it is possible to generate a pair of reciprocal polyhedra $\boldsymbol{P}, \boldsymbol{P}'$ that produces a pair of reciprocal form and force diagrams $\boldsymbol{F}, \boldsymbol{F}'$ when projected onto the plane. These diagrams follow the duality of $\boldsymbol{P}, \boldsymbol{P}'$ (Figure 1b) and thus form vertices v map to force faces f' while form edges e map to force edges e'. Consequently, the static equilibrium of each node of $\boldsymbol{F}$ is represented by a closed force polygon in $\boldsymbol{F}'$. At the same time, the axial stress of every edge in e is visually depicted by the edge length of the reciprocal edges e'. Likewise, 3D trusses in static equilibrium can be regarded as projections of 4-polytopic 4D stress functions,[17] where a construction analogous to the one described above can be used for finding the force reciprocals of polyhedral spatial trusses in static equilibrium. For a more in-depth discussion on these reciprocal constructions in the context of contemporary graphic statics, the reader is pointed to Konstantatou et al.[1]

As illustrated in Figure 2, a form and a force diagram can be further combined to generate a Minkowski Sum, a diagram that can be interpreted as a visual representation of Maxwell's load path theorem[17,18]:

$$\sum F_T L_T - \sum F_C L_C = \sum \vec{P_i}.\vec{r_i} \tag{2}$$

where $\sum F_T L_T$ is the tension load path of the structure, with F_T and L_T respectively the axial force and the length of edge e_T in tension; $\sum F_C L_C$ is the compression load path of the structure, with F_C and L_C respectively the axial force and the length of edge e_C in compression; $\sum \vec{P_i} \cdot \vec{r_i}$ is the sum of the dot products of the external force $\vec{P_i}$ and the position vector $\vec{r_i}$ of $\vec{P_i}$, with respect to an arbitrary origin.

2.2 | Strut-and-tie models and stress fields in reinforced concrete structures

Strut-and-tie and stress field models are particularly useful for visualizing the flow of internal forces and stresses

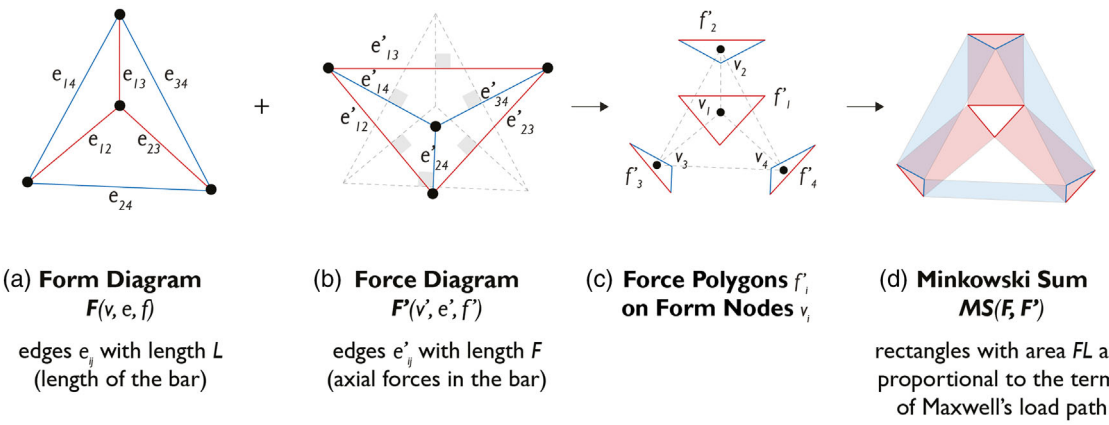

FIGURE 2 (a) Form diagram $\boldsymbol{F}(v, e, f)$ of a 2D truss where the lengths L of the edges e represent the lengths of the bars of the truss. (b) Reciprocal force diagram $\boldsymbol{F}'(v', e', f')$ of $\boldsymbol{F}$ where the lengths F of the edges e' represent the corresponding axial forces in the bars of the truss (red-tension, blue-compression). The form and force diagrams $\boldsymbol{F}, \boldsymbol{F}'$ are represented in the Maxwell configuration and thus the pairs of reciprocal edges e, e' are perpendicular to each other. (c) Force faces f' are scaled and vectorially added with their reciprocal form vertices v. (d) Diagrams $\boldsymbol{F}, \boldsymbol{F}'$ can be scaled and combined in the form of a Minkowski Sum $\boldsymbol{MS}(\boldsymbol{F}, \boldsymbol{F}')$. This can be achieved by adding the closed force polygons—triangles in this instance—to their reciprocal form vertex. As the areas of the rectangles of this hybrid diagram are proportional to FL, the Minkowski Sum represents Maxwell's load path theorem visually[17,18]

within structural elements. These engineering models can be effectively used for the analysis and design of reinforced concrete structures.[19] They are directly related to each other, as they rely on the lower bound theorem of the theory of plasticity (Figure 3).

Around the turn of the 19th century, Ritter[20] and Mörsch[21] introduced an innovative approach for the analysis of reinforced concrete beams subjected to shear and bending.[22] According to their proposal, a loaded reinforced concrete beam develops an internal load-bearing system in the form of a truss, whose elements are subjected to either tension or compression. This truss analogy has been further refined by Rausch,[23] Kupfer,[24] Leonhardt,[25] and Thürlimann et al.,[26] among others. Strut-and-tie models were introduced by Schlaich et al.[27] as a generalization of the above truss analogy model,[22] to describe the mechanical behavior of those regions in reinforced concrete structures with static and geometric discontinuities. In this approach, strut-and-tie models in reinforced concrete were derived with the help of elastic stress trajectories, generated through Finite Element Analysis.[27,28] A different application of strut-and-tie models in cracked reinforced concrete was then proposed by Muttoni et al.[19] based on the *lower bound theorem* of the theory of plasticity.[29–31] In the last decades, several computational frameworks have been presented to automate the generation of strut-and-tie models, mostly based on topology optimisation[32–34] or finite element analysis.[35,36]

Stress field models can be used for the analysis and design of reinforced concrete structures. As well as helping to identify appropriate reinforcement configurations, stress fields can be used to characterize the distribution of stresses in concrete compression struts. Besides this, they are especially suitable for the design of reinforced concrete elements, the description of regions of discontinuity and the morphology of concrete nodes.[19,37] In the last few years, various approaches for the automatic generation of 2D discrete and continuous stress fields have been proposed.[36,38–40] Moreover, a direct connection between 2D discrete stress fields and the reciprocal form and force diagrams of graphic statics has been highlighted in several occasions.[17–19] Nevertheless, no

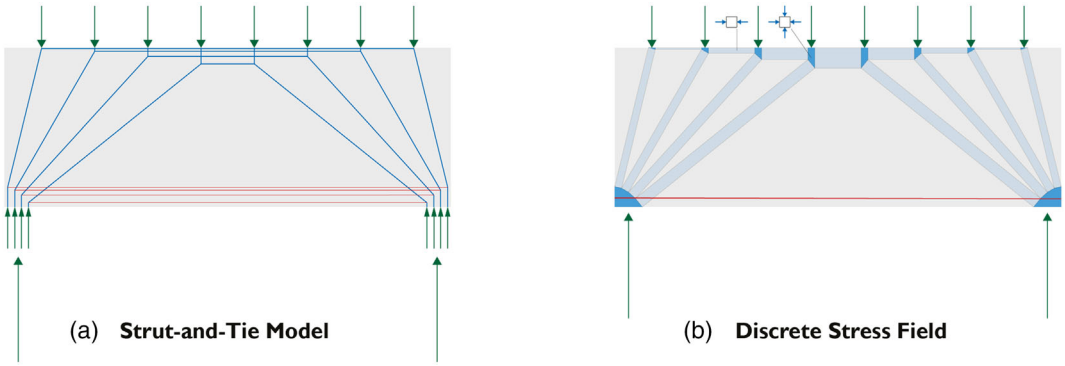

FIGURE 3 (a) Strut-and-tie model of a reinforced concrete beam (red-tension, blue-compression, green-external force). (b) Discrete stress field derived from the strut-and-tie model as shown in (a): compression stresses are resisted by concrete struts, while the longitudinal reinforcement resists the tensile stresses. The strut-and-tie model can be considered as a synthetic representation of the stress field, in which only the stress resultants are represented

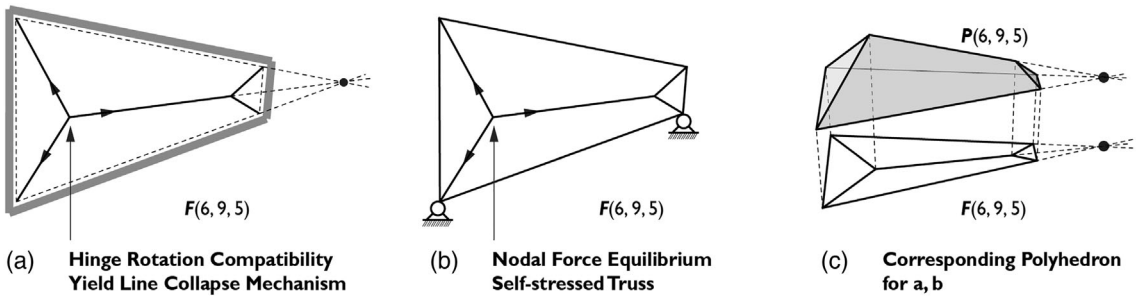

FIGURE 4 Equivalence between the compatibility of a yield line mechanism (a) and the static equilibrium state of a self-stressed truss (b). Both are projections of a polyhedral Airy stress function (c). Adapted from[44]

direct mathematical procedure for the generation of discrete and continuous stress fields that can also be generalized to 3D has been introduced until now.

2.3 | Yield lines in reinforced concrete slabs

Yield line theory makes it possible to assess the load capacity of reinforced concrete slabs using the *upper bound theorem* of plasticity. In a two-dimensional reinforced concrete slab, a yield line pattern can be created that generates rigid regions of concrete, which define a compatible collapse mechanism. As suggested by Moy,[41] however, the evaluation of the compatibility of the mechanism is not straight-forward. In line with the "static geometric analogies" proposed by Calladine,[42] Denton[43] introduced a systematic procedure to address this question. Following this approach, it is possible to establish an analogy between a 2D yield line pattern and a 2D truss, where the yield lines defining the mechanism correspond to the bars of the truss. Based on this set-up, the yield line pattern defines a compatible collapse mechanism if and only if the corresponding truss is self-stressed, and it is in static equilibrium.[43] This truss analogy suggests that the number of degrees of freedom (DoF) of a yield line mechanism in a slab is equal to the number of self-stress states in the corresponding truss. As highlighted by Williams and McRobie,[44] the truss analogy described above can be related to graphic statics via the Airy stress function. In this regard, a yield line mechanism in a slab is compatible if and only if it is a projection of a plane-faced polyhedron (Figure 4). This considering that its corresponding two-dimensional self-stressed truss is necessary a projection of a polyhedral stress function.

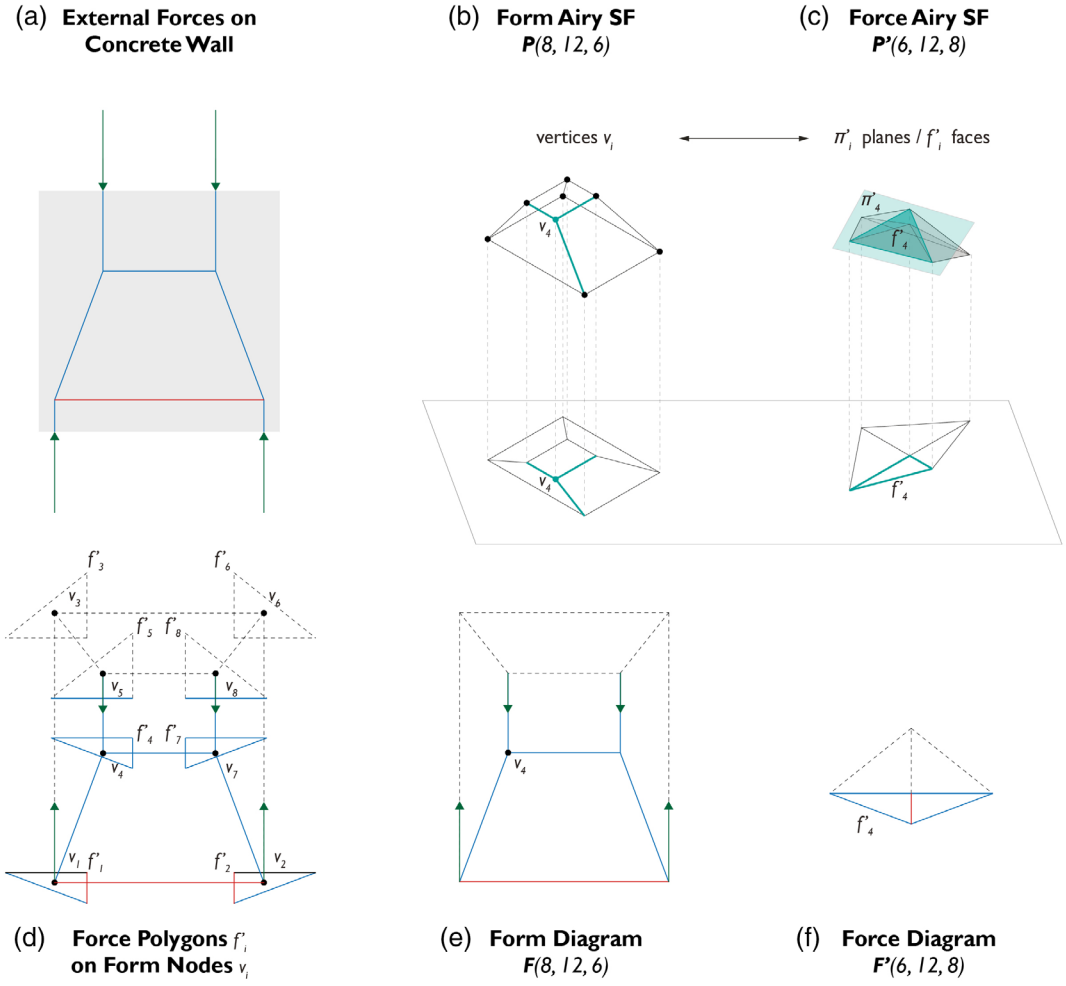

FIGURE 5 (a) External forces and reactions on a concrete wall for a simple case of a strut-and-tie model. (b, c) Corresponding pair of reciprocal polyhedral Airy stress functions $\boldsymbol{P}(8, 12, 6)$, $\boldsymbol{P}'(6, 12, 8)$. The duality between vertices v_i in $\boldsymbol{P}$ and faces f'_i in $\boldsymbol{P}'$ is highlighted. The projection of $\boldsymbol{P}$ and $\boldsymbol{P}'$ onto the plane results in a pair of reciprocal form $\boldsymbol{F}$ and force $\boldsymbol{F}'$ diagrams. In particular, form nodes v_i in $\boldsymbol{F}$ map to closed force polygons f'_i in $\boldsymbol{F}'$ (d) hence guaranteeing static equilibrium

3 | DIRECT GEOMETRICAL APPROACH FOR GENERATING STRESS FIELDS AND YIELD LINES

3.1 | Discrete stress fields

This section presents the proposed geometrical framework for the generation of discrete stress fields in reinforced concrete structures grounded on the use of graphic statics' form and force diagrams and reciprocal stress functions (Section 2.1). For a given topology of a strut-and-tie network, a 2D discrete stress field within a given boundary of material can be generated based on the following approach:

- At first, the geometric input parameters are defined: the topology of the 2D strut-and-tie network; the geometric boundary constraints; the magnitude, direction

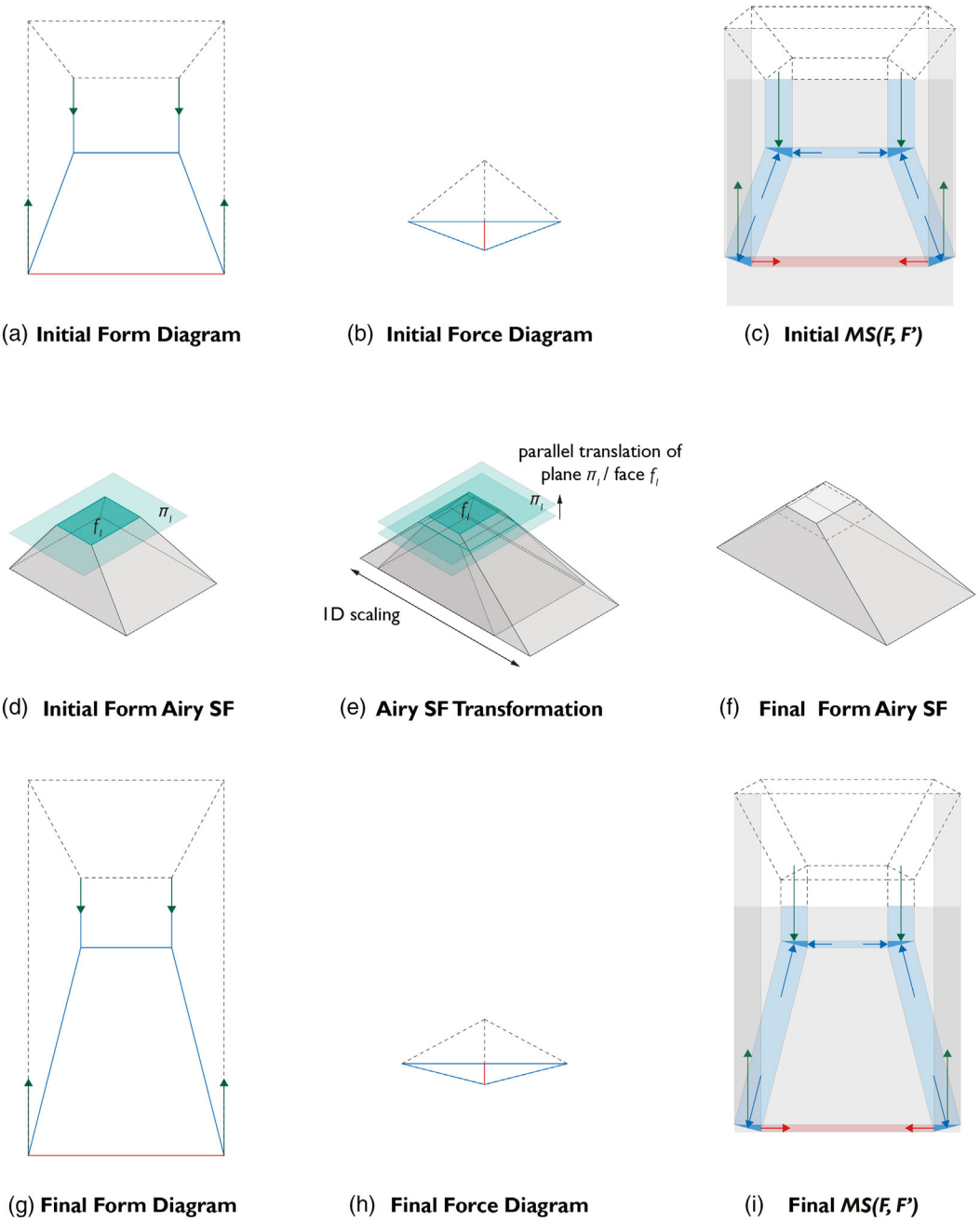

FIGURE 6 (a) Initial form diagram of the given strut-and-tie network (FIGURE 5a). (b) Corresponding initial force diagram. (c) Initial Minkowski Sum as a generic discrete stress field. (d) Initial form Airy stress function. (e) Transformation of the Airy stress function in terms of 1D scaling and parallel translation of the plane defining the top face. (f) Final form Airy stress function. (g) Corresponding final form diagram. (h) Corresponding final force diagram. (i) Final Minkowski Sum as a generic discrete stress field which conforms to the given geometric boundary, material strength, and external forces

and points of application of the external forces (Figure 5a).

- An initial 2D form diagram $\boldsymbol{F}(v, e, f)$ is defined following the same topology of the strut-and-tie network (Figure 5e). The external forces in the initial strut-and-tie network are replaced by an auxiliary sub-structure to produce an overall equivalent self-stressed configuration. It should be noted that this initial 2D form diagram need not be in static equilibrium.
- The initial 2D form diagram (Figure 5e) is then lifted to the third dimension to create its corresponding 3D polyhedral Airy stress function (Figure 5b). If the 2D form diagram is not in static equilibrium, then it is not a projection of a plane-faced polyhedron.[5] In this case, after imposing the planarity of the faces in the polyhedral Airy stress function, the position of the vertices will be adjusted at the same time. Hence, the projected geometry of the 2D form diagram is also modified accordingly to achieve static equilibrium. The geometry of the polyhedral Airy stress function provides the designer with intuitive and visual information on the structural behavior of the strut-and-tie model. Specifically, a strut in compression corresponds to two adjacent faces forming a ridge (locally convex) whereas a tensile tie corresponds to adjacent faces forming a valley (locally concave).
- The polyhedral stress function $\boldsymbol{P}$ is then mapped via a polar transformation to its reciprocal $\boldsymbol{P}'$ (Figure 5c) as explained in Section 2.1. The orthogonal projection of this pair of reciprocal polyhedra onto the 2D plane yield a pair of reciprocal form and force diagrams $\boldsymbol{F}$, $\boldsymbol{F}'$ in a Maxwell 2D configuration (Figure 5b,c,e,f). In fact, to each vertex of the form diagram corresponds a face (closed force polygon) in the force diagram (Figure 5d).
- $\boldsymbol{F}$, $\boldsymbol{F}'$ (Figure 6a,b) are then combined into a 2D Minkowski Sum (Figure 6c), which is topologically

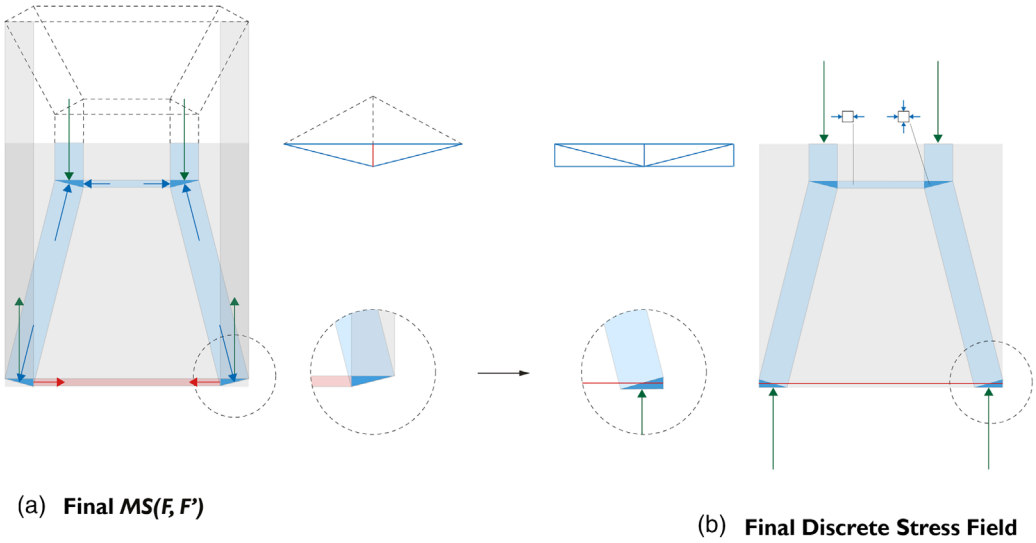

FIGURE 7 Transformation of the nodal geometry of the generic stress field (a) to accommodate for the presence of tensile reinforcement in the final discrete stress field (b). This solution can be regarded as a starting point for further detailed design[19]

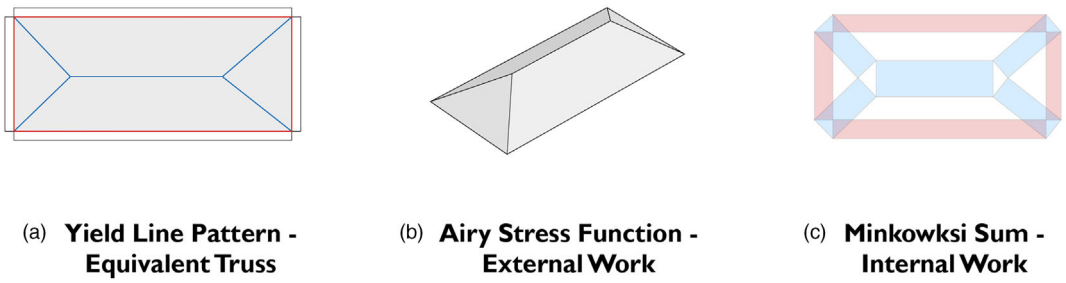

FIGURE 8 (a) 2D geometry of a simple case of a yield line pattern in terms of a form diagram $\boldsymbol{F}(6, 9, 5)$. (b) Corresponding polyhedral Airy stress function $\boldsymbol{P}(6,9,5)$ representing visually the external work. (c) Combination of $\boldsymbol{F}$ and $\boldsymbol{F}'$ as Minkowski sum representing visually the internal work

identical to a discrete stress field. In fact, the Minkowski Sum is an instance of a valid stress field with a uniform hydrostatic stress-state. The Minkowski Sum is compatible with the magnitudes and directions of the given external forces (Figure 5a) while the application points of the forces can be different from the initial input (Figure 6c).

- After applying specific constraint-based geometric transformations to the polyhedral Airy stress function related to the initial 2D form diagram, such as parallel translations of the planes containing the polyhedral faces (Figure 6d–f), the corresponding Minkowski Sum can be manipulated whilst the form and force diagrams are updated (Figure 6g,h). These transformations aim to adjust the 2D Minkowski Sum in relation to the specified material strength, which is reflected in the width of the compression struts, and until it matches the given geometric boundary (Figure 6i), while retaining the magnitudes, directions and lines of action of the external forces. These constraints require that the dihedral angles between adjacent faces related to the external forces remain unaltered during these transformations. It should be highlighted that in the typical but straightforward case of 2D strut-and-tie models where the applied loads are vertical, the allowed operations also include global affine transformations such as 1D scaling.
- To derive an appropriate stress field from the Minkowski Sum, the nodal geometry of this diagram (Figure 7a) needs to be transformed to accommodate for the presence of tensile reinforcement. In fact, under the assumption that all the nodes of the stress field have a hydrostatic state of stress, the proposed method can be directly applied to compression-only cases

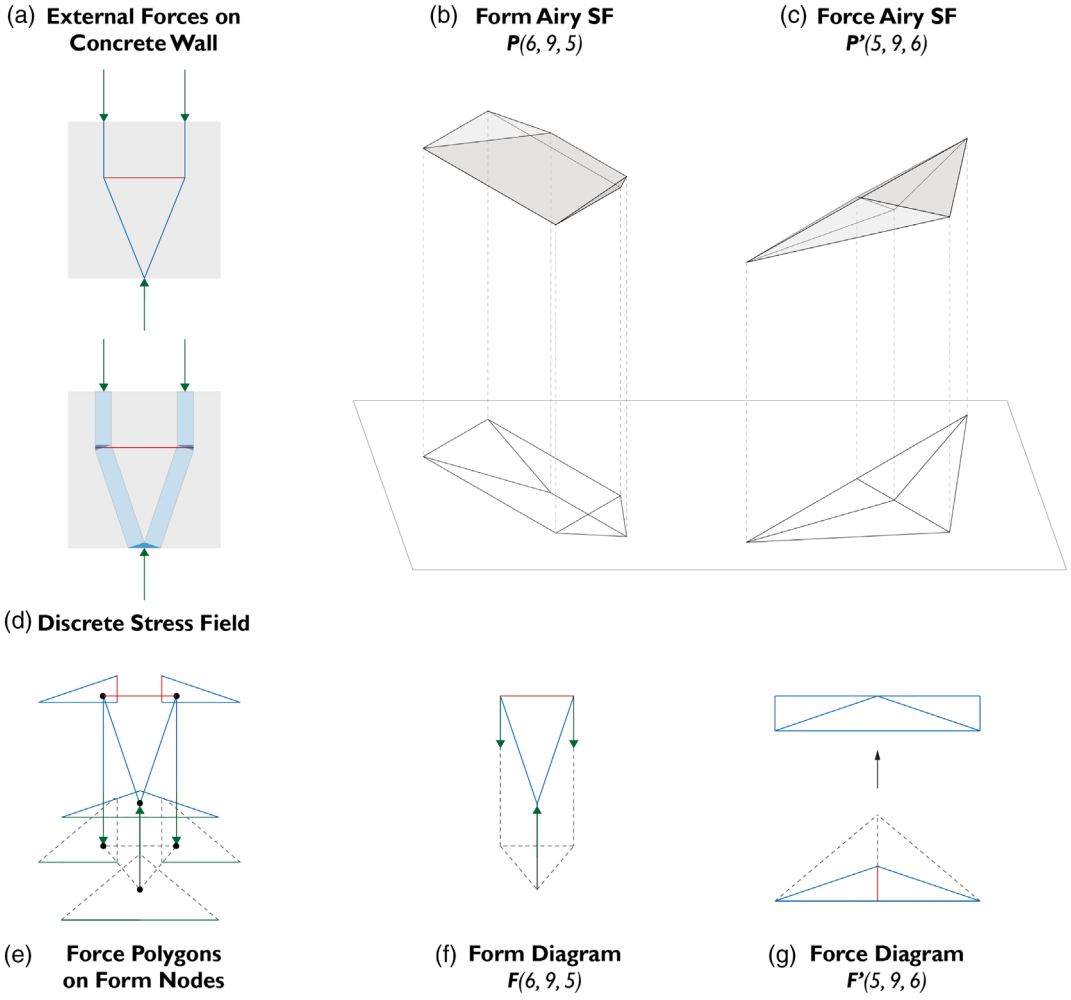

FIGURE 9 (a) External forces and reactions on a concrete wall for a case study of a strut-and-tie model. (b, c) Corresponding pair of reciprocal polyhedral Airy stress functions $\boldsymbol{P}(6, 9, 5)$, $\boldsymbol{P}'(5, 9, 6)$ and their projections in terms of form and force diagrams $\boldsymbol{F}(6, 9, 5)$, $\boldsymbol{F}'(5, 9, 6)$ (f, g). Every face—closed force polygon—of the force diagram corresponds to a form node (e) hence guaranteeing static equilibrium. (d) Resulting final discrete stress field

(i.e., CCC nodes). Hence, the corresponding force diagram has to be adjusted in those nodes in which concrete struts are equilibrated by reinforcement bars (i.e., CCT and CTT nodes). In these cases, it is possible to ensure appropriate anchorage of the reinforcement after modifying the order of the edges in the force polygons. After adjusting the nodal geometry (Figure 7b), the Minkowski Sum becomes an acceptable solution of a discrete stress field for the specified applied loads, boundary conditions, material strength and input strut-and-tie topology. This solution should be regarded as a starting point for the further detailed design of the reinforcement layout and the nodal zones.[19]

3.2 | Yield line patterns

In analogy to the approach of generating discrete stress fields explained in the previous section, it is also possible to define yield line patterns using form and force diagrams and reciprocal stress functions (Section 2.1).

This geometrical method can be used to check for compatibility of the mechanism while providing an intuitive and straightforward representation of the internal and external work. The proposed method is grounded in the following steps:

- The input parameters are initially defined: 2D geometry of the hinge lines of the proposed mechanism,

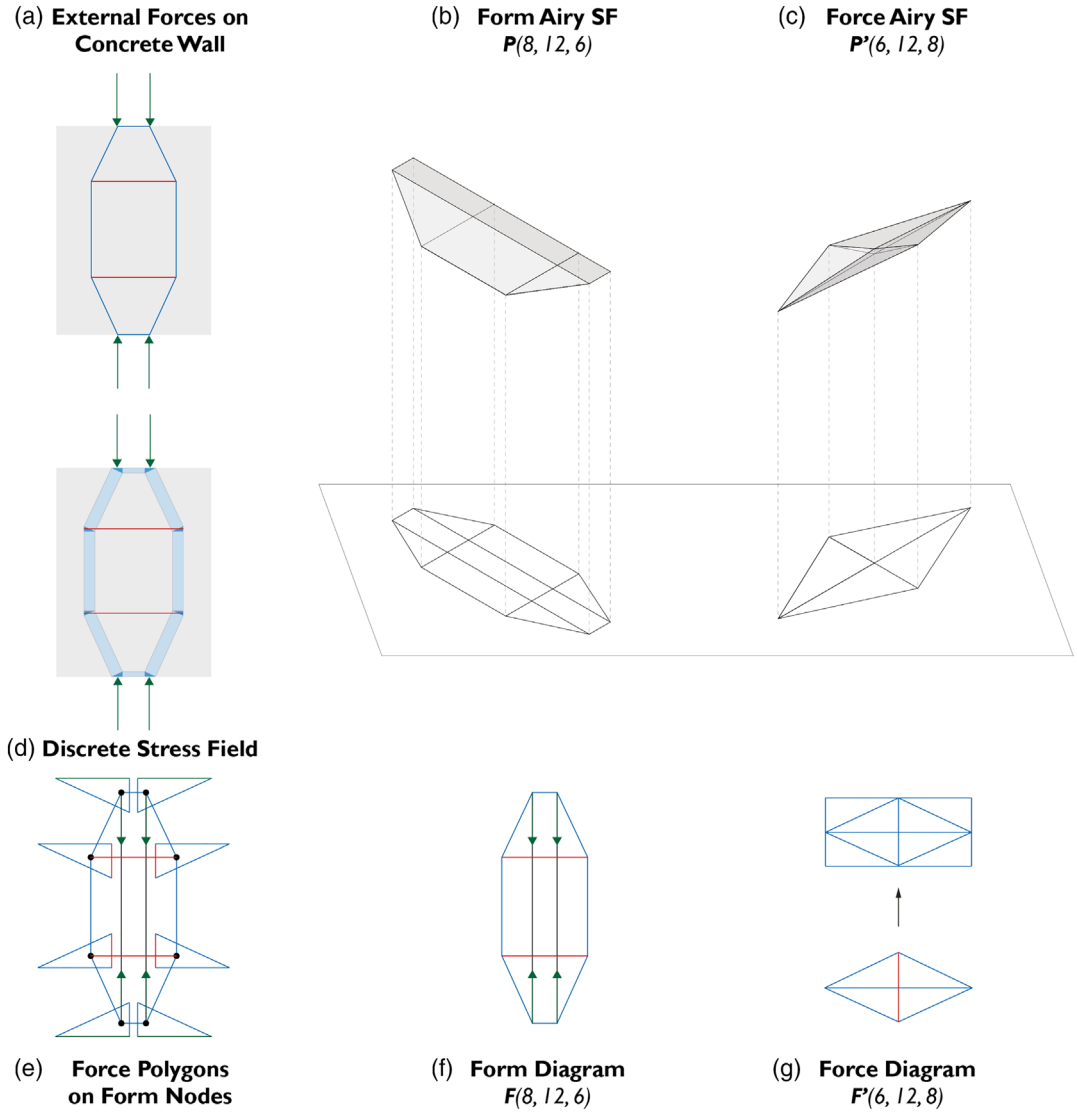

FIGURE 10 (a) External forces and reactions on a concrete wall for a case study of a strut-and-tie model. (b, c) Corresponding pair of reciprocal polyhedral Airy stress functions $\boldsymbol{P}(8, 12, 6)$, $\boldsymbol{P'}(6, 12, 8)$ and their projections in terms of form and force diagrams $\boldsymbol{F}(8, 12, 6)$, $\boldsymbol{F'}(6, 12, 8)$ (f, g). Every face—closed force polygon—of the force diagram corresponds to a form node (e) hence guaranteeing static equilibrium. (d) Resulting final discrete stress field

which gives the underlying truss geometry $\boldsymbol{F}(v, e, f)$ (Figure 8a).

- A check is performed to assess if a plane-faced polyhedron is generated when $\boldsymbol{F}$ is lifted up one dimension to create the corresponding polyhedral Airy stress function $\boldsymbol{P}(v, e, f)$ (Figure 8b). If this is the case, $\boldsymbol{F}(v, e, f)$ corresponds to a compatible yield line mechanism. If it is not the case, the planarity of the faces of the Airy stress function is imposed. The angles between adjacent faces of $\boldsymbol{P}(v, e, f)$ are defined so that they are equal to the rotational angles between adjacent rigid regions of the mechanism in $\boldsymbol{F}(v, e, f)$. The polyhedral Airy stress function $\boldsymbol{P}'(v', e', f')$ reciprocal to $\boldsymbol{P}(v, e, f)$ is then generated via a polar transformation. The projection of $\boldsymbol{P}'(v', e', f')$ onto the plane then generates $\boldsymbol{F}'(v', e', f')$, which represents a compatible mechanism.
- By combining $\boldsymbol{F}$ and $\boldsymbol{F}'$, the related Minkowski Sum diagram (Figure 8c) can be constructed. The areas of the rectangular faces of this diagram are proportional to the product of lengths of the yield lines and the corresponding rotational angles.

Once multiplied by the plastic moment of resistance per unit length, which is here assumed to be uniform, the areas of the rectangles in the Minkowski Sum diagram gives a geometrical representation of the internal work W_I. In this representation (Figure 8c), the blue rectangles denote the work of compressive members enclosed from the red rectangles denoting the work of tensile members at the boundary. W_I is expressed by Moy[41] with Equation 3 and is the integral over all yield lines, of the rotation angle θ_i multiplied

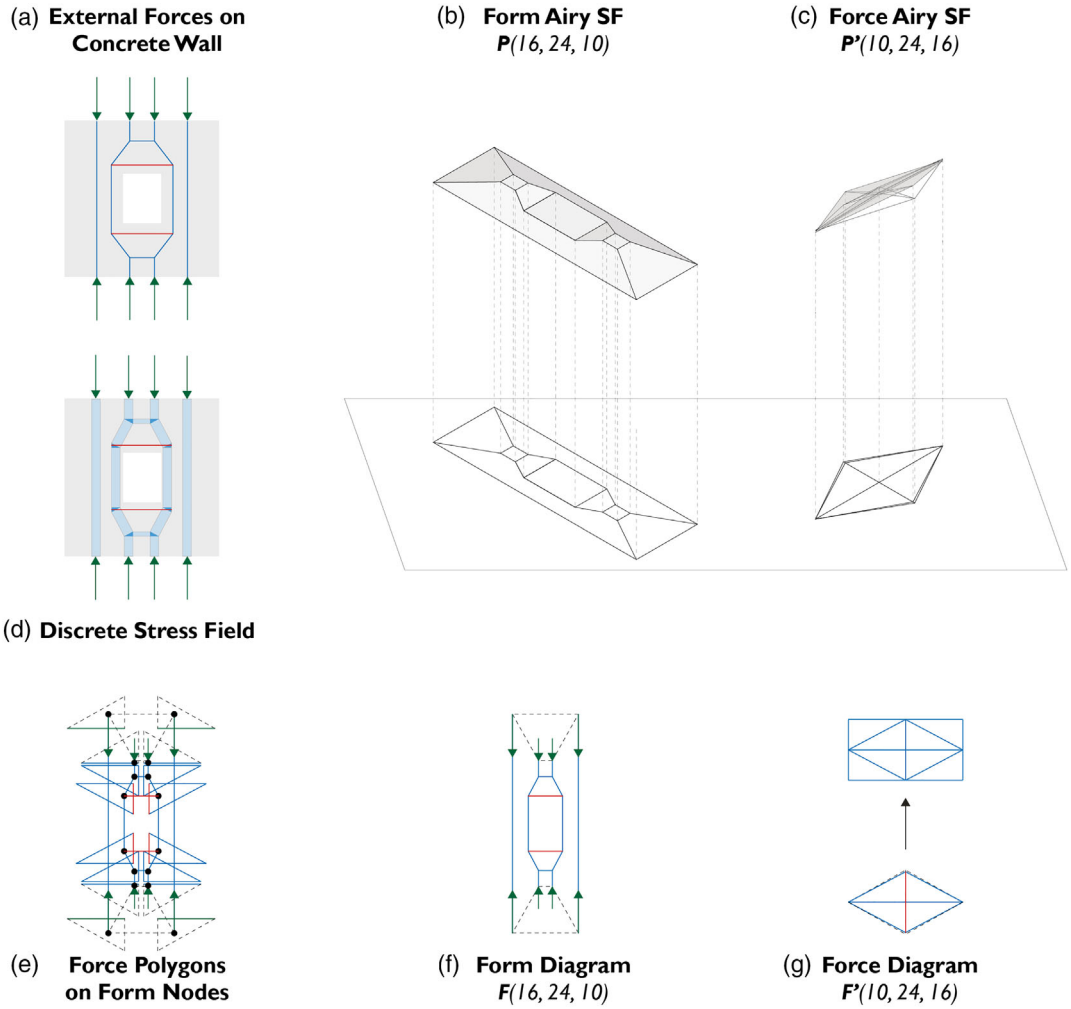

FIGURE 11 (a) External forces and reactions on a concrete wall for a case study of a strut-and-tie model. (b, c) Corresponding pair of reciprocal polyhedral Airy stress functions $\boldsymbol{P}(16, 24, 10)$, $\boldsymbol{P}'(10, 24, 16)$ and their projections in terms of form and force diagrams $\boldsymbol{F}(16, 24, 10)$, $\boldsymbol{F}'(10, 24, 16)$ (f, g). Every face—closed force polygon—of the force diagram corresponds to a form node (e) hence guaranteeing static equilibrium. (d) Resulting final discrete stress field

by the total plastic moment of resistance M_i transverse to the yield line.

The external work W_E is expressed by Equation 4[41] and is the integral over all the rigid regions, of the load q_i applied on each element multiplied by its corresponding displacement Δ_i. Thus, for a uniformly distributed load q, W_E is the volume of the polyhedral Airy stress function multiplied by the q, where Δ is the height of the stress function.

$$W_I = \sum \left[\theta_i \int_S M_i ds \right] \tag{3}$$

$$W_E = \sum \left[\int_A q_i \Delta_i dA \right] \tag{4}$$

Then the general expression of the work equation is:

$$\sum \left[\int_A q_i \Delta_i dA \right] = \sum \left[\theta_i \int_S M_i ds \right] \tag{5}$$

over all the rigid regions and every yield line. That is, the (weighted) volume of the Airy stress function is equated with (weighted) surface areas of rectangular regions of the Minkowski Sum.

Generally, concrete slabs have a 2-directional reinforcement which most commonly is perpendicular. The equation of the plastic moment of resistance per unit length M_n is then given by[41]:

$$M_n = M \sin^2 \theta' + \mu M cos^2 \theta' \tag{5}$$

where μ denotes different resistance moments and θ' the angle of the yield line with respect to the direction of the reinforcement. If $\mu = 1$ the reinforcement is isotropic and $M_n = M$.

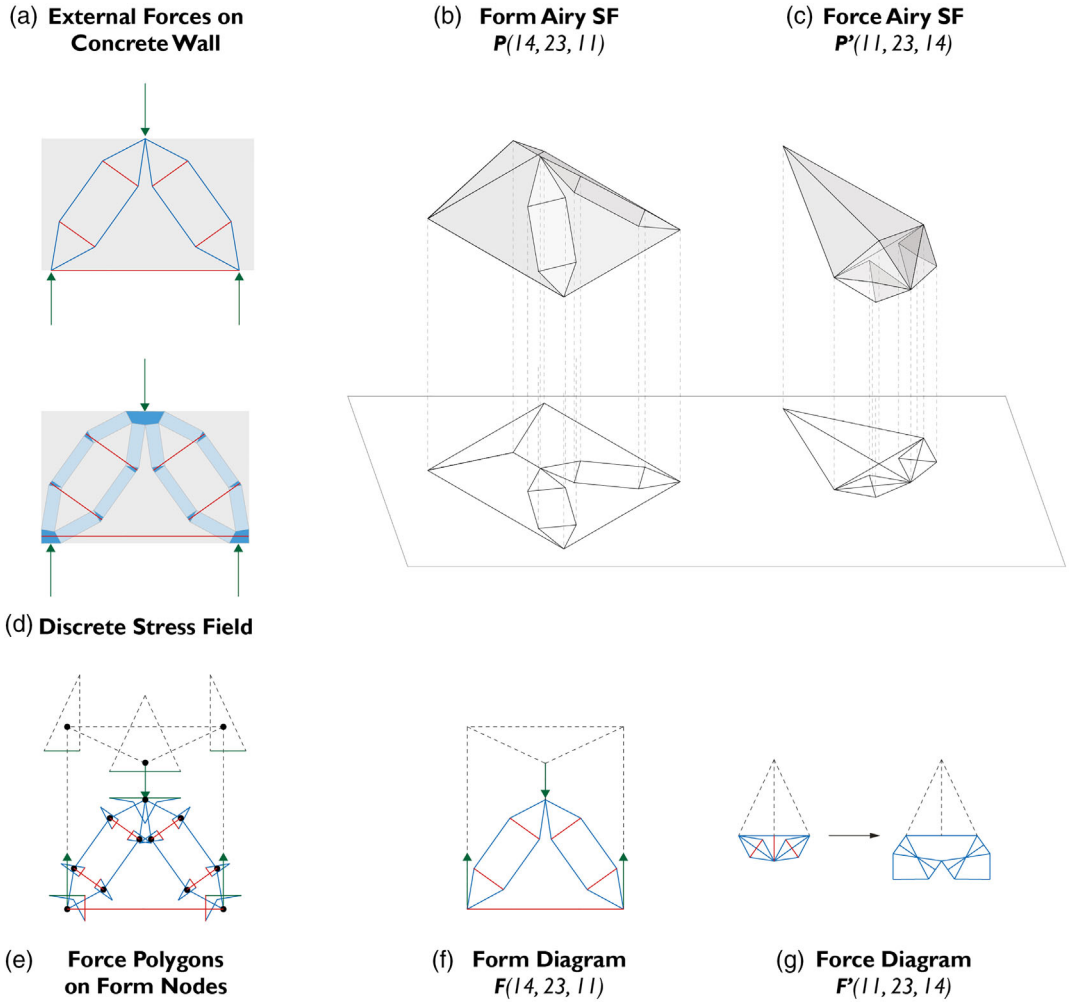

FIGURE 12 (a) External forces and reactions on a concrete wall for a case study of a strut-and-tie model. (b, c) Corresponding pair of reciprocal polyhedral Airy stress functions ***P***(*14*, *23*, *11*), ***P'***(*11*, *23*, *14*) and their projections in terms of form and force diagrams ***F***(*14*, *23*, *11*), ***F'***(*11*, *23*, *14*) (f, g). Every face—closed force polygon—of the force diagram corresponds to a form node (e) hence guaranteeing static equilibrium. (d) Resulting final discrete stress field

In this case, the internal work is the same as the total surface area of the Minkowski Sum multiplied by the scalar M. If $\mu \neq 1$ then for the geometrical analogy between the Minkowski Sum and the internal work to hold, the rectangles should be scaled 1-dimensionally in the plane by a factor of $\sin^2\theta' + \mu\cos^2\theta'$ and perpendicular to the yield lines.

4 | APPLICATIONS AND EXTENSIONS

4.1 | Discrete stress fields in 2D

In the following examples, the geometric procedure described in Section 3.1 is used to generate discrete stress fields in reinforced concrete for various specified strut-and-tie topologies, geometric boundaries and applied loads (Figures 9–12). For each case, a self-stressed form diagram equivalent to the input strut-and-tie topology (Figures 9a, 10a, 11a, and 12a) is created by replacing the external forces with an auxiliary sub-structure (Figures 9f, 10f, 11f, and 12f). Then, the internal vertices of this initial form diagram are lifted to create a plane-faced polyhedral Airy stress function (Figures 9b, 10b, 11b, and 12b). This is mapped to its reciprocal polyhedron (Figures 9c, 10c, 11c, and 12c) which in turn is projected orthogonally on the 2D plane to reveal the 2D force diagram (Figures 9g, 10g, 11g, and 12g) each face—force polygon—of which corresponds to a form node (Figures 9e, 10e, 11e, and 12e); thus guaranteeing global static equilibrium. To develop a valid stress field which conforms to the given boundary conditions, material strength, and external forces, the polyhedral Airy stress function is adjusted through basic geometric transformations. In this way, the final stress field (Figures 9d, 10d, 11d, and 12d) can be adapted to the given design requirements. This stress field can be used as a base for further detailed design.

The same procedure applied above can be used for the development of a valid stress field of a beam with

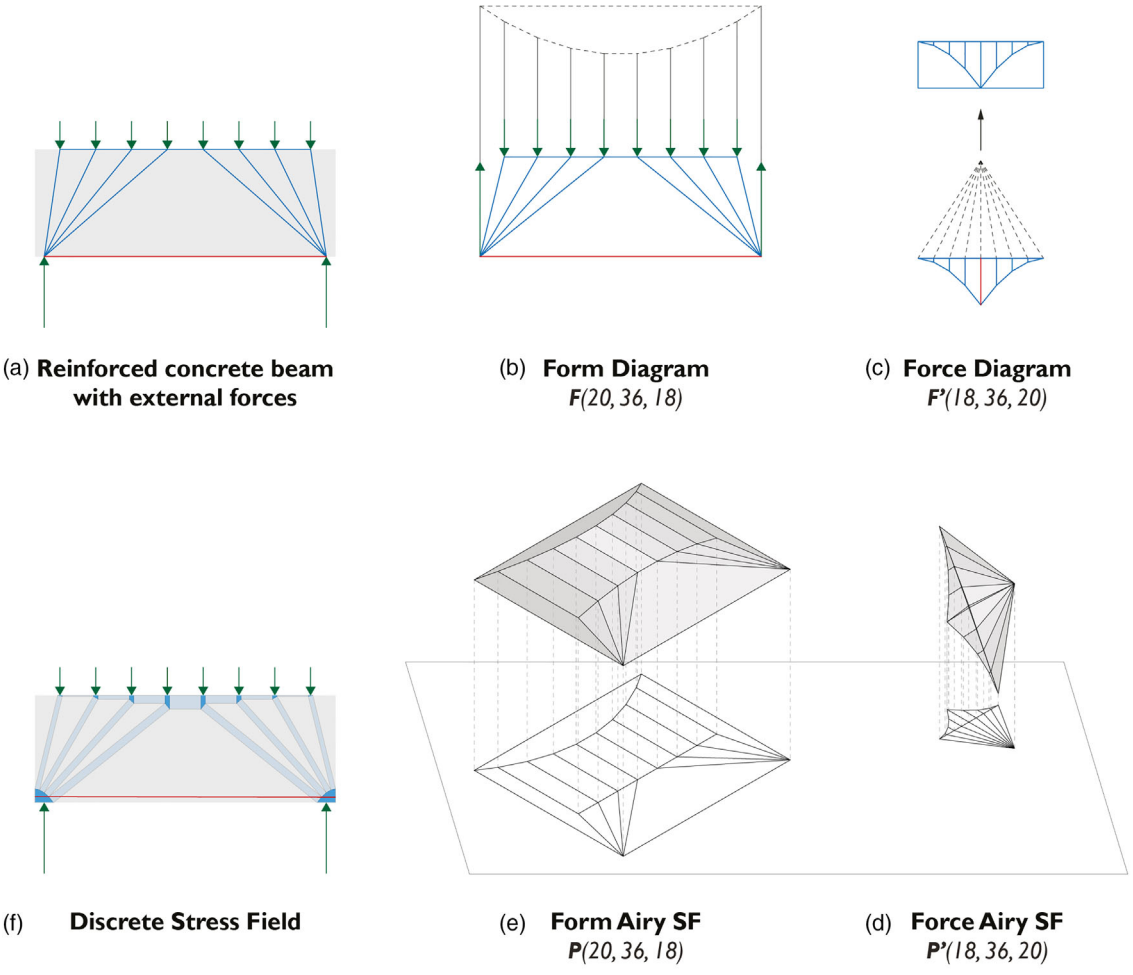

FIGURE 13 (a) Initial strut-and-tie network for a concrete beam with multiple concentrated loads. (b) Equivalent geometry of a self-stressed truss $\boldsymbol{F}(20, 36, 18)$. (c) Reciprocal force diagram $\boldsymbol{F'}(18, 36, 20)$. (d) Polyhedral stress function of the force diagram $\boldsymbol{P'}(18, 36, 20)$. (e) Polyhedral stress function of the form diagram $\boldsymbol{P}(20, 36, 18)$. (f) Resulting discrete stress field

multiple concentrated loads (Figure 13). In this case, it can be noticed that the initial simplified strut-and-tie network (Figure 14a) has fewer vertices than the final strut-and-tie network (Figure 14b) since some of the nodes of the former become clusters of nodes in the latter. In fact, the nodal axial forces in the initial strut-and-tie network are

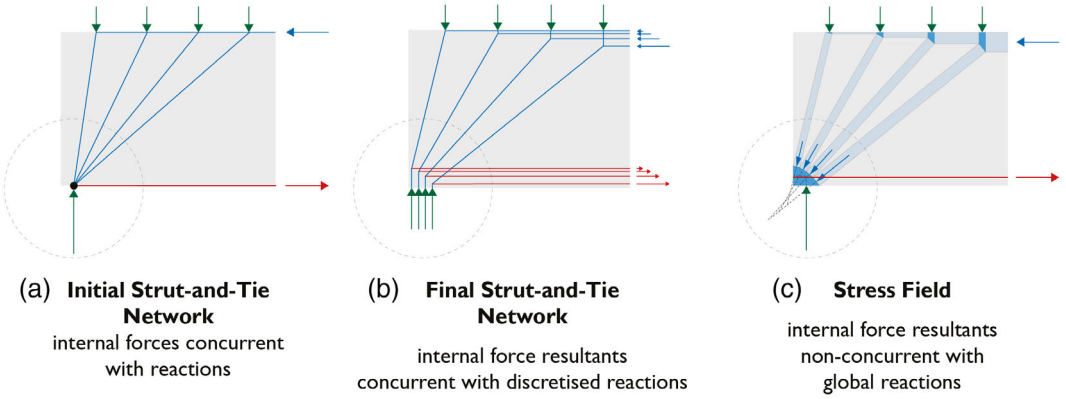

FIGURE 14 (a) The nodal axial forces in the initial strut-and-tie network are concurrent. (b) On the contrary, in the case of the final strut-and-tie network, the nodal axial forces are not concurrent due to the geometry of the node in the discrete stress field (c)

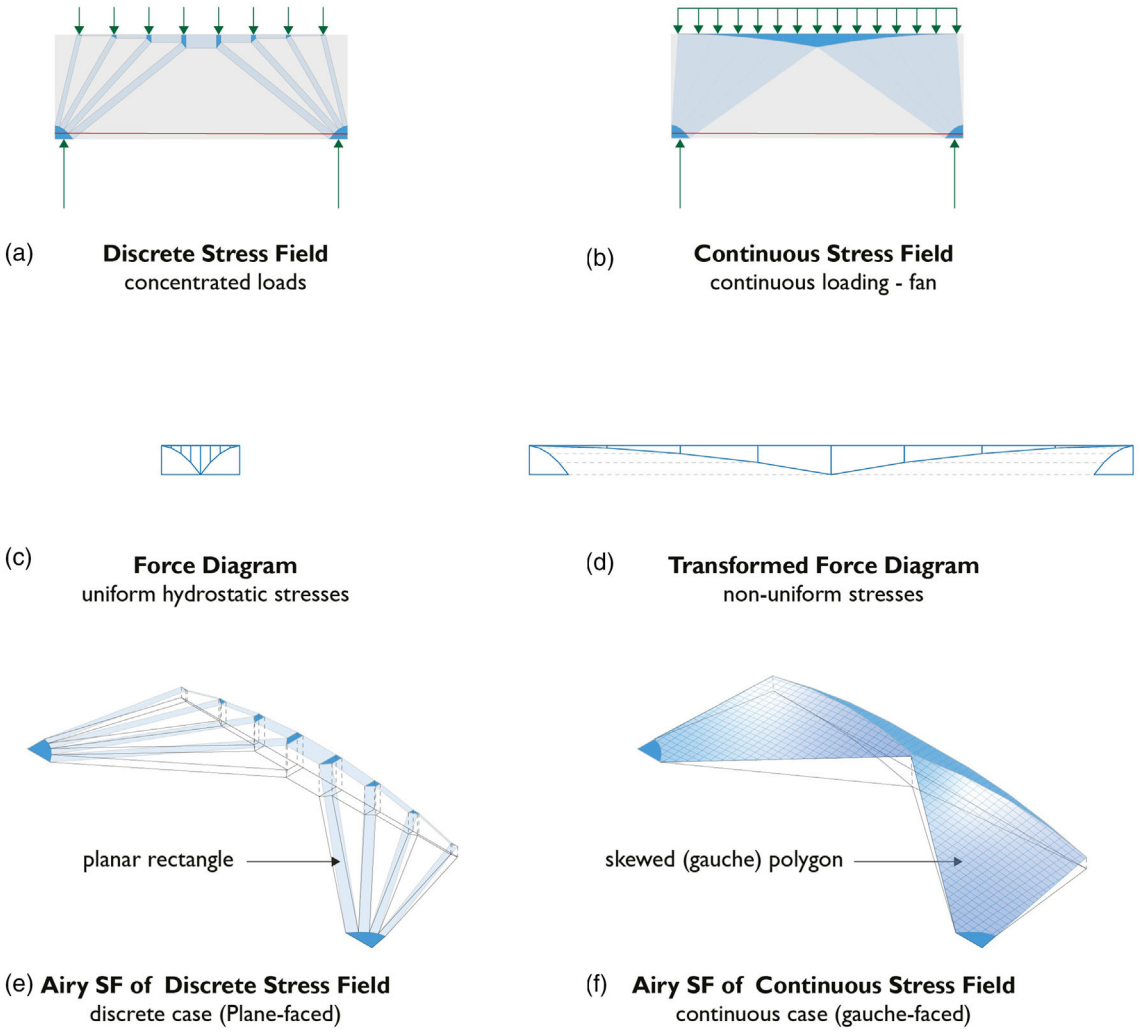

FIGURE 15 (a) Discrete Airy stress function for uniform hydrostatic stresses under concentrated loading. (b) Continuous Airy stress function for nonuniform stresses under continuous loading. (e, f) Transformation of the stress field between concentrated and continuous loading and corresponding changes in the force diagram for nonuniform stresses

concurrent, while they are not concurrent in the final strut-and-tie network generated through the proposed approach, although they are in equilibrium. This discrepancy is directly related to the geometry of the nodal elements in the corresponding discrete stress field (Figure 14c).

4.2 | Continuous stress fields in 2D

Stress fields in reinforced concrete can be continuous with the internal stress resultant nonperpendicular to the nodes (Figure 15). It should be highlighted how the Airy stress function behaves geometrically differently in the two cases of discrete and continuous loading (Figure 15a,b). In the case of discrete loading and uniform hydrostatic pressure, the Airy stress function over the stress field comprises plane-faced rectangles (Figure 15e). The change of slope between adjacent geometrical elements gives the magnitude of the force resultants, and each rectangle represents a uniaxial stress field in the beam. In the limit case of continuous loading, a nonuniform biaxial stress distribution emerges. The biaxial nonuniform stress is translated to gauche polygons (Figure 15f)—that is, skew polygons whose vertices do not lie on the same plane[5]—and the surface spanning them is curved. Any such surface is admissible, and it will correspond to a different biaxial state of self-stress. Thus, the continuous limit introduces shear, other than the axial forces of the discrete solution, with the circular symmetric fan with no transverse stresses as a particular case. In the general case of continuous loading, the Airy stress function can be described as a surface ϕ—rather than the polyhedral version $\boldsymbol{P}$ used in graphic statics for trusses—for which the known Cauchy stress components can be calculated.[15]

4.3 | Discrete stress fields in 3D

Three-dimensional stress fields can be easily generated by extending the approach described in

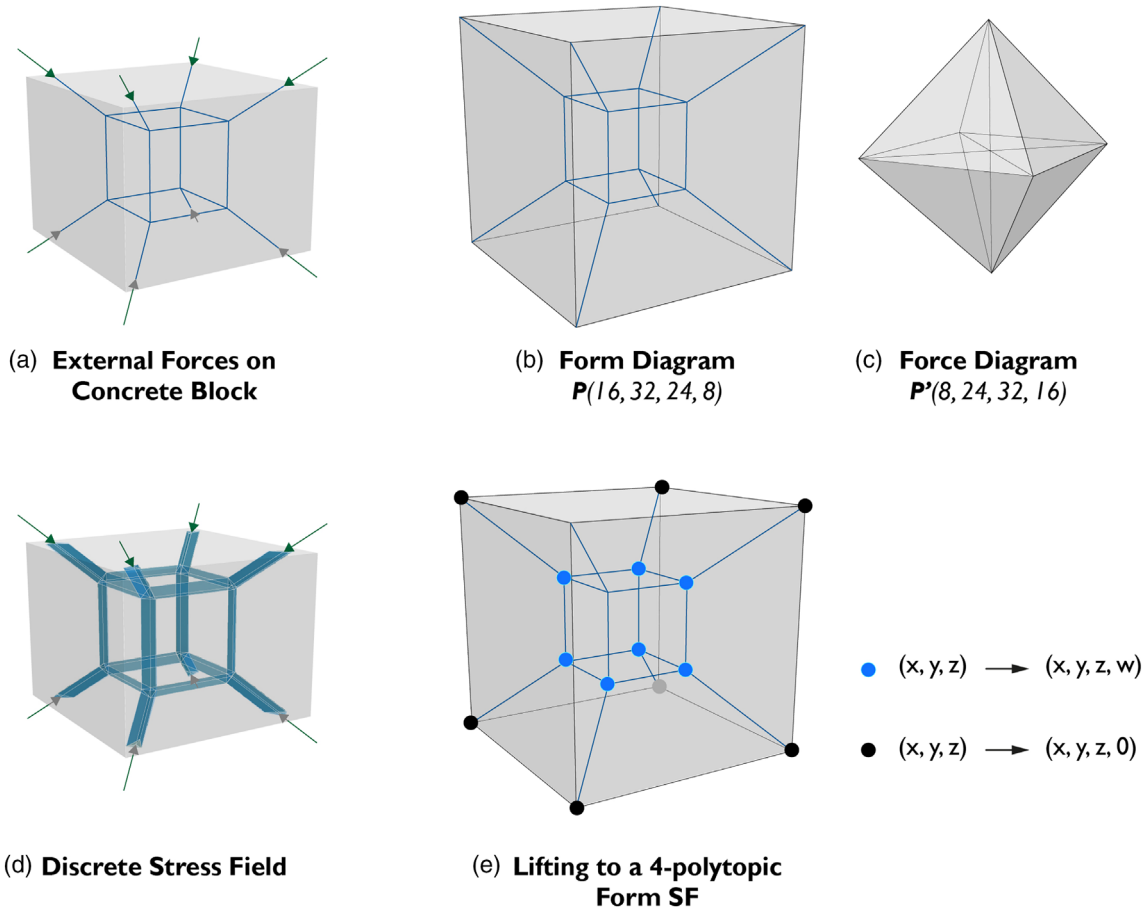

FIGURE 16 (a) A common 3D strut-and-tie model for a cubic concrete block. (b) Corresponding form diagram as a polyhedral spatial truss. (c) Reciprocal Rankine 3D force diagram. (d) Resulting discrete 3D stress field derived from a spatial Minkowski Sum. (e) Polyhedral form diagram, transformed into the 4-polytopic stress function by lifting its internal nodes to 4D

Section 3.1 to the third dimension. As illustrated in Figure 16, the form diagram (Figure 16b) of a 3D strut-and-tie model within a given concrete block (Figure 16a) can be lifted to 4D space to generate a plane-faced 4-polytopic stress function (Figure 16e). When projected back to 3D space, its reciprocal 4-polytopic stress function generates a Rankine 3D reciprocal force diagram (Figure 16c). By combining 3D form and force diagrams, it is possible to obtain a 3D Minkowski Sum, which defines a uniform hydrostatic stress field in the boundary of the concrete block (Figure 16d).

4.4 | Yield lines in 2D

The approach described in Section 3.2 is used here to produce yield lines for specific examples reported in the literature (Figure 17). The analogous truss configuration is first identified for each example (Figure 17a). The polyhedral Airy stress function can then be used to test the compatibility of the mechanism while offering a geometric interpretation of the external work (Figure 17b). The Minkowski Sum can be eventually constructed (Figure 17c), while providing a geometric representation of the internal work.

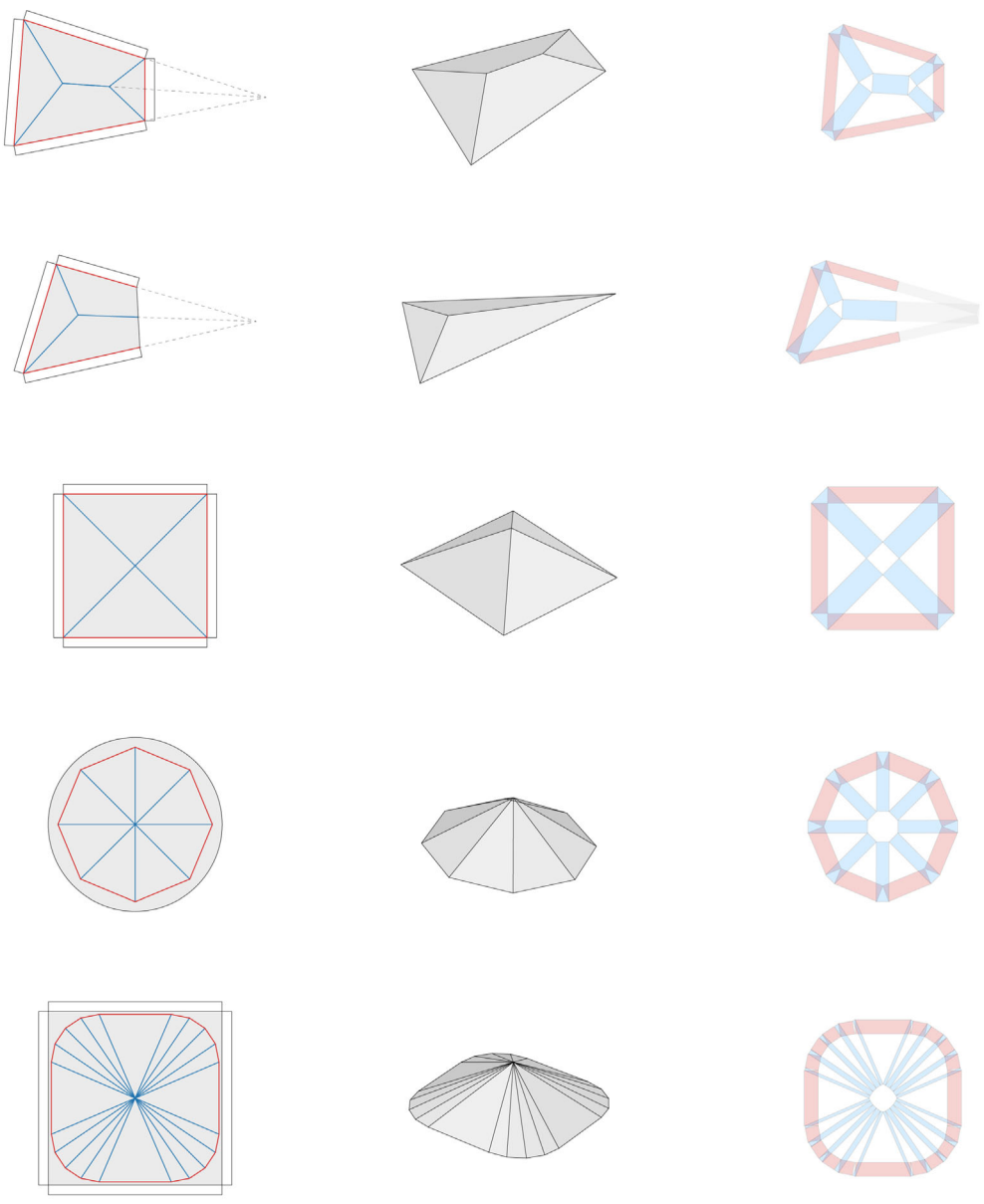

FIGURE 17 (a) Common cases of yield line patterns. (b) Corresponding polyhedral Airy stress functions used for checking the compatibility of the mechanisms while providing a visual interpretation of the external work. (c) Corresponding Minkowski Sums giving an intuitive representation of the internal work

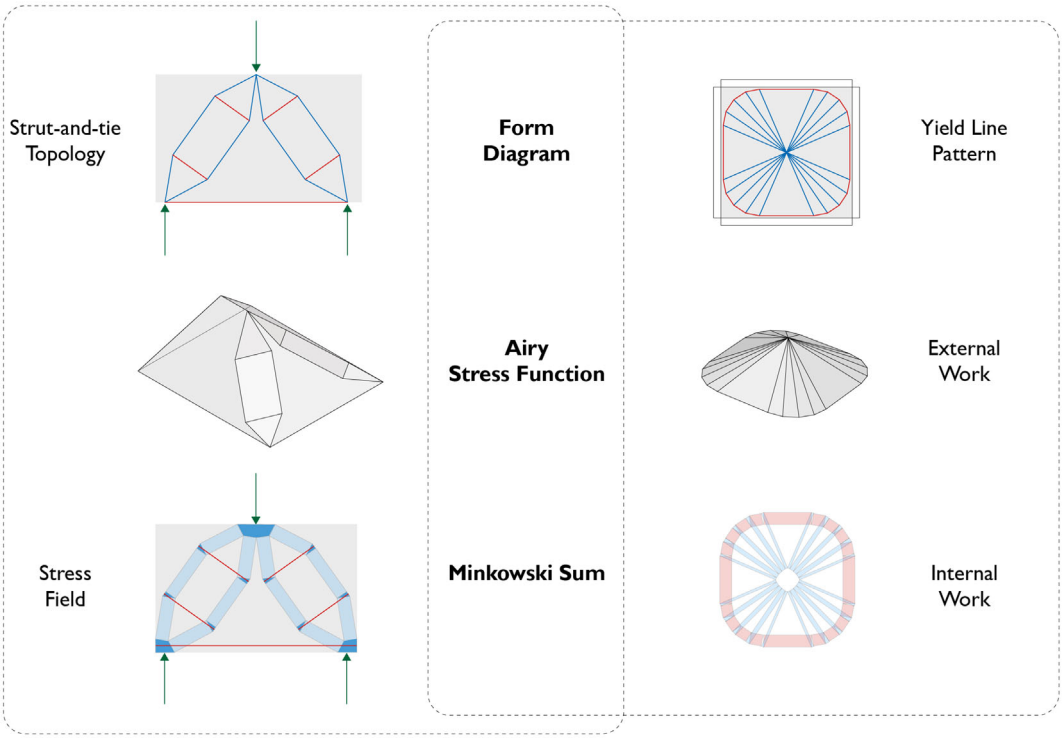

FIGURE 18 Overview of the proposed approach, showing how the same geometrical method, based on graphic statics' form and force diagrams, and reciprocal stress functions, can be used for the definition of both stress fields and yield line patterns in reinforced concrete

5 | CONCLUSION

This article has highlighted the potential of graphic statics and its associated geometrical constructions as a design and analysis tool for the direct creation of discrete 2D and 3D stress fields, and compatible yield line mechanisms in reinforced concrete structures (Figure 18). Through the proposed approach, it has been shown how several important engineering problems related to reinforced concrete can be solved using reciprocal polyhedral Airy stress functions. This approach thus provides researchers and designers with novel, visual and intuitive design and analysis capabilities.

From a theoretical standpoint, it can be observed that the same unified geometrical approach introduced in this article can be employed to generate both stress fields and yield lines in reinforced concrete, although they are respectively based on the lower bound and upper bound theorems of the theory of plasticity. Notwithstanding their simplicity, the methods described in this article are highly efficient and competitive in comparison to more conventional numerical approaches, in the sense that they are visual, straightforward and can be conveniently implemented and utilized for both analysis and design.

ACKNOWLEDGMENTS

The authors are grateful for fruitful conversations with Bill Baker and for feedback received during the International fib Symposium on Conceptual Design of Structures in Madrid—September 2019. MK was a recipient of an EPSRC studentship through the University of Cambridge when this research project was developed. PD and JS receive salaries from ETH Zürich. FAM receives a salary from the University of Cambridge. The authors thankfully acknowledge the Engineering and Physical Sciences Research Council for funding this research through the EPSRC Centre for Doctoral Training in Future Infrastructure and Built Environment (EPSRC grant reference number EP/L016095/1).

CONFLICT OF INTEREST

The authors declare no potential conflicts of interest with respect to the research, authorship and/or publication of this research.

DATA AVAILABILITY STATEMENT

Data sharing not applicable to this article as no datasets were generated or analysed during the current study.

ORCID

Marina Konstantatou https://orcid.org/0000-0003-0593-9407

REFERENCES

1. Konstantatou M, D'Acunto P, McRobie A. Polarities in structural analysis and design: n-dimensional graphic statics and structural transformations. Int J Solids Struct. 2018;152–153: 272–293.
2. Konstantatou M, D'Acunto P, McRobie A, Schwartz J. Applications of graphic statics to analysis and design of reinforced concrete: Stress fields and yield lines. Proceedings of the International Fib Symposium on Conceptual Design of Structures, Madrid; 2019.
3. Cremona L. Le Figure Reciproche nella Statica Grafica. Milano, Tipografia Giuseppe Bernardoni: Tipografia di Giuseppe Bernardoni, 1872.
4. Culmann K. Die Graphische Statik. Zurich: Meyer und Zeller, 1866.
5. Maxwell JC. On reciprocal figures, frames and diagrams of forces. Philos Mag. 1864;27:250–261.
6. Rankine M. Principle of the equilibrium of polyhedral frames. Lond Edinb Dublin Philos Mag J Sci. 1864;27:92.
7. Akbarzadeh M, Van Mele T, Block P. On the equilibrium of funicular polyhedral frames and convex polyhedral force diagrams. Comput-Aided Des. 2015;63 (suppl C: 118–128.
8. Block P, Ochsendorf J. Thrust network analysis: A new methodology for three-dimensional equilibrium. J Int Assoc Shell Spatial Struct. 2007;48:167–173.
9. D'Acunto P, Jasienski J-P, Ohlbrock PO, Fivet C, Schwartz J, Zastavni D. Vector-based 3D graphic statics: A framework for the design of spatial structures based on the relation between form and forces. Int J Solids Struct. 2019; 167:58–70.
10. Fivet C. Projective transformation of structural equilibrium. Int J Space Struct. 2016;31:135–146.
11. Mazurek A, Beghini A, Carrion J, Baker WF. Minimum weight layouts of spanning structures obtained using graphic statics. Int J Space Struct. 2016;31:112–120.
12. McRobie A. The geometry of structural equilibrium. R Soc Open Sci. 2017;4(3):160759. https://doi.org/10.1098/rsos.160759.
13. Mitchell T, Baker W, McRobie A, Mazurek A. Mechanisms and states of self-stress of planar trusses using graphic statics, part I: The fundamental theorem of linear algebra and the Airy stress function. Int J Space Struct. 2016;31: 85–101.
14. Airy GB. On the strains in the interior of beams. Philos Trans R Soc Lond. 1862;153:49–79.
15. Timoshenko S, Goodier JN. Theory of elasticity. New York: McGraw-Hill Book Company, Inc, 1951.
16. Maxwell JC. On reciprocal figures, frames, and diagrams of forces. Trans R Soc Edinb. 1870;7:160–208.
17. McRobie A. Maxwell and Rankine reciprocal diagrams via Minkowski sums for two-dimensional and three-dimensional trusses under load. Int J Space Struct. 2016;31: 203–216.
18. Zanni G, Pennock GR. A unified graphical approach to the static analysis of axially loaded structures. Mech Mach Theory. 2009;44:2187–2203.
19. Muttoni A, Schwartz J, Thürlimann B. Design of concrete structures with stress fields. Basel: Birkhäuser, 1997.
20. Ritter W. Die Bauweise Hennebique (The Hennebique System). Schweizerische Bauzeitung. 1899;23(7):41–61.
21. Mörsch E. Der Eisenbetonbau. Seine Theorie Und Anwendung. 3rd ed. Stuttgart: Verlag Konrad Wittwer, 1908.
22. Kurrer KE. The history of the theory of structures, from arch analysis to computational mechanics. Berlin: Ernst & Sohn, 2008.
23. Rausch E. Berechnung des Eisenbetons gegen Verdrehung (Torsion) und Abscheren. 2nd ed. Berlin: Springer, 1938.
24. Kupfer H. Erweiterung der Mörschschen Fachwerkanalogie mit Hilfe des Prinzips vom Minimum der Formänderungsarbeit, CIB-Bulletin 40; 1964.
25. Leonhardt F. Reducing the shear reinforcement in reinforced concrete beams and slabs. Mag Concr Res. 1965;17(53): 187–198.
26. Thürlimann B, Marti P, Pralong J, Ritz P, Zimmerli B. Vorlesung zum Fortbildungskurs für Bauingenieure (Advanced lecture for civil engineers). ETH Zürich: Institut für Baustatik und Konstruktion, 1983.
27. Schlaich J, Schäfer K, Jennewein M. Toward a consistent design of structural concrete. PCI J. 1987;32:74–150.
28. Schlaich J. Strut-and-tie model design of structural concrete. IABSE congress report, 14; 1992.
29. Drucker DC. On structural concrete and the theorems of limit analysis. Int Assoc Bridge Struct Eng (IABSE). 1961; 21:49–59.
30. Gvozdev AA. The determination of the value of the collapse load for statically indeterminate systems undergoing plastic deformation. Int J Mech Sci. 1960;1:322–335.
31. Prager W, Hodge PG. Theory of perfectly plastic solids. New York: John Wiley & Sons, Inc, 1951.
32. Ali MA, White RN. Automatic generation of truss model for optimal design of reinforced concrete structures. ACI Struct J. 2001;98:431–442.
33. Bruggi M. Generating strut-and-tie patterns for reinforced concrete structures using topology optimization. Comput Struct. 2009;87:1483–1495.
34. Liang QQ, Xie YM, Steven GP. Topology optimization of strut-and-tie models in reinforced concrete structures using an evolutionary procedure. ACI Struct J. 2000;97: 322–332.
35. Biondini F, Bontempi F, Malerba PG. Stress path adapting strut-and-tie models in cracked and uncracked R.C. elements. Struct Eng Mech. 2001;12:685–698.
36. Muttoni A, Fernández RM, Niketic F. Design versus assessment of concrete structures using stress fields and strut-and-tie models. ACI Struct J. 2015;112:605–616.
37. Nielsen MP, Hoang LC. Limit analysis and concrete plasticity. Boca Raton: CRC Press, 2011.
38. Hajdin R. Computerunterstützte Berechnung von Stahlbetonscheiben mit Spannungsfeldern. Zürich: [PhD thesis]. ETH Zürich, 1990.
39. Kostic N. Computer-based development of stress fields. Presented at the *6th International PhD Symposium in Civil Engineering*, Zürich; 2006.
40. Mata-Falcón J, Tran DT, Kaufmann W, Navrátil J. Computer-aided stress field analysis of discontinuity concrete regions. Proceedings of the Conference on Computational Modelling of Concrete and Concrete Structures (EURO-C 2018), 641–650; 2018.

41. Moy SSJ. Plastic methods for steel and concrete structures. Hong Kong: The MacMillan Press Ltd, 1981.
42. Calladine CR. Theory of shell structures. New York: Cambridge University Press, 1983.
43. Denton SR. Compatibility requirements for yield-line mechanisms. Int J Solids Struct. 2001;38:3099–3109.
44. Williams C, McRobie A. Graphic statics using discontinuous Airy stress functions. Int J Space Struct. 2016;31:121–134.

AUTHOR BIOGRAPHIES

Marina Konstantatou,
Department of Engineering,
University of Cambridge,
Cambridge, UK.
Email: mk822@cam.ac.uk

Pierluigi D'Acunto,
ETH Zürich, Institute of Technology in Architecture, Chair of Structural Design,
Zürich, Switzerland.
Email: dacunto@arch.ethz.ch

Allan McRobie,
Department of Engineering,
University of Cambridge,
Cambridge, UK.
Email: fam@eng.cam.ac.uk

Joseph Schwartz,
ETH Zürich, Institute of Technology in Architecture, Chair of Structural Design,
Zürich, Switzerland.
Email: schwartz@arch.ethz.ch

How to cite this article: Konstantatou M, D'Acunto P, McRobie A, Schwartz J. Unified geometrical framework for the plastic design of reinforced concrete structures. *Structural Concrete*. 2020;1–19. https://doi.org/10.1002/suco.201900440